LAB.II/BT/74-2
26 June 1974

ELASTIC STRESS WAVES IN MATTER DUE TO RAPID HEATING BY AN INTENSE HIGH-ENERGY PARTICLE BEAM

P. Sievers

ABSTRACT

The absorption of intense high-energy proton bursts of several microseconds duration causes a considerable temperature increase of the same rise-time inside the intercepted material. During this short period, thermal expansion of the irradiated material is partly prevented by its mass inertia. This gives rise to dynamic stresses which propagate through the material with the velocity of sound.

In this report the dynamic stresses are calculated under ideally elastic conditions where Hook's law is strictly valid. In particular, one-dimensional stress waves in slender rods and circular waves in disks and cylinders are studied. Simple expressions are given to estimate the maximum possible dynamic stresses in targets and absorber blocks as a function of the burst duration and the applied temperature field.

G E N E V A

1974

CONTENTS

1. INTRODUCTION

The heating of materials exposed to intense high-energy particle beams is a well-known phenomenon which has to be taken into account in the construction of targets and beam absorbers used in high-energy accelerators. In addition to the purely thermal effects, stresses are created by the rapid non-uniform temperature increase inside the material. Since the duration of the particle bursts available from accelerators is of the order of microseconds or even shorter, the heating of the irradiated material proceeds in times during which heat conduction may be neglected and where the mass inertia, which resists the thermal expansion, becomes important.

The elastic stress waves produced by the latter effect have been studied by Bargmann[1] for the case of a uniformly and rapidly heated rod on the basis of Laplace transforms. Experimental work has been performed by Avery et al.[2] with an electron beam of 50 nsec duration.

In this report the elastic stress waves in a thin rod will shortly be treated on the basis of Fourier series, which leads to simple analytic expressions.

In addition, cylindrical stress waves originating in the centres of disks and cylinders are studied with the help of Fourier-Bessel series. In these cases characteristic differences compared with the case of longitudinal waves must be expected. The investigation of cylindrical geometries is of particular importance for the design of the dump blocks required for the absorption of the beam of the CERN Super Proton Synchrotron (SPS).

In the following calculations, ideal elastic materials are assumed, where Hook's law is strictly valid. If, however, the temperature rise inside the irradiated body is sufficiently high, so that the material becomes partly plastic, more sophisticated methods using the theory of shock waves in dispersive media must be applied.

2. LONGITUDINAL STRESS WAVES IN A THIN ROD

2.1 Instantaneous temperature rise

Considering the one-dimensional problem we assume, as in Ref. 1, a freely suspended thin elastic rod of length 2L, whose temperature is instantaneously increased by T_0 uniformly over the total rod, remaining constant thereafter. The equation of motion for the axial stress is given by:

$$\frac{\partial^2 \sigma_0(x,t)}{\partial x^2} = \frac{1}{c^2} \frac{\partial^2 \sigma_0(x,t)}{\partial t^2} \,. \tag{1}$$

The velocity c of compressional one-dimensional elastic waves is given by:

$$c = \sqrt{\frac{E}{\rho}} ,$$

where E is the modulus of elasticity and ρ the mass density.

For the evaluation of the initial stress $\sigma_0(x,0)$ we assume that the sudden temperature rise T_0 does not produce any thermal expansion at time t = 0. Then the rod is only submitted to a compressive stress of

$$\sigma_0(x,0) = E\alpha T_0 \quad \text{for } |x| < L ,$$

where α is the linear coefficient of thermal expansion.

Since the rod is freely suspended, the stresses must remain zero at the end faces at any time:

$$\sigma_0(L,t) = \sigma_0(-L,t) = 0, \qquad 0 \leq t.$$

In Fig. 1 the initial stress distribution along the rod is shown. In addition, we assume that the velocity of the stress wave at the time t = 0 is zero:

$$\left.\frac{\partial \sigma_0(x,t)}{\partial t}\right|_{t=0} = 0 . \tag{3}$$

Now we can proceed with the usual ansatz:

$$\sigma_0(x,t) = E\alpha T_0 \sum_{n=0}^{\infty} a_n(x) \cos \omega_n t , \tag{4}$$

where the initial and boundary conditions must be satisfied by the proper choice of the functions $a_n(x)$ and the frequencies ω_n. The initial distribution of the stress at t = 0 is given by the appropriate part of a square wave shown in Fig. 2, which is represented by the following Fourier series:

$$f(x) = \frac{4}{\pi} \sum_{n=0}^{\infty} \frac{(-1)^n}{(2n+1)} \cos (2n+1) \frac{\pi x}{2L} \tag{5}$$

so that the functions a_n are given by

$$a_n(x) = \frac{4}{\pi} \frac{(-1)^n}{(2n+1)} \cos (2n+1) \frac{\pi x}{2L} . \tag{6}$$

The introduction of the ansatz (4) into the wave equation (1) gives a condition for the permitted frequencies ω_n, and with the boundary condition (2) one obtains

$$\omega_n = \pi(2n+1) \frac{c}{2L} . \tag{7}$$

Thus we arrive at the final expression for the stresses as a function of position x and time t:

$$\sigma_0(x,t) = E\alpha T_0 \frac{4}{\pi} \sum_{n=0}^{\infty} \frac{(-1)^n}{(2n+1)} \cos\left[(2n+1)\frac{\pi x}{2L}\right] \cos\left[(2n+1)\frac{c\pi}{2L}t\right] . \qquad (8)$$

The product of the two trigonometric functions can be transformed into their sum, i.e.

$$\sigma_0(x,t) = E\alpha T_0 \frac{2}{\pi} \sum_{n=0}^{\infty} \frac{(-1)^n}{(2n+1)} \left\{\cos\frac{(2n+1)\pi}{2L}(x+ct) + \cos\frac{(2n+1)\pi}{2L}(x-ct)\right\} . \qquad (9)$$

This represents the expected result of two identical "fundamental" waves travelling in opposite directions, where the fundamental wave is given by

$$F(x) = \frac{2}{\pi} \sum_{n=0}^{\infty} \frac{(-1)^n}{(2n+1)} \cos(2n+1)\frac{\pi x}{2L} , \qquad (10)$$

which is of course again a square wave as shown above in Fig. 2, with the amplitude reduced by a factor of 2.

With the abbreviation (10) the stresses can be written in the very compact form:

$$\sigma_0(x,t) = E\alpha T_0 \left\{F(x+ct) + F(x-ct)\right\} \qquad (11)$$

and the stresses can easily be obtained by graphical superposition of the fundamental waves. Obviously the maximum stresses have the value $\pm E\alpha T$. The development of the stress in time, obtained by this method, is illustrated in Fig. 3.

2.2 Finite rise-time of the temperature jump

The more realistic case of a finite rise-time of the temperature increase, produced by a particle pulse of duration t_0, can now be easily derived from the solution given in Section 2.1. The stresses for this case are given by

$$\sigma(x,t) = \int_0^t \sigma_0(x,t-\tau) \frac{\partial \bar{T}(\tau)}{\partial \tau} d\tau , \qquad (12)$$

where $\sigma_0(x,t)$ is the stress for an instantaneous temperature rise given by Eq. (9), $\bar{T}(t)$ is the normalized temperature increase as a function of time, and τ is the variable of integration.

We assume a linear temperature rise as given in Fig. 4:

$$\bar{T}(t) = \begin{cases} t/t_0 & 0 \le t \le t_0 \\ 1 & t > t_0 \end{cases} \tag{13}$$

which is produced by a constant particle flux of duration t_0.

Introducing Eq. (8) into Eq. (12) gives, after integration, for $0 \le t \le t_0$:

$$\sigma_i(x,t) = \frac{E\alpha T_0}{t_0} \frac{4}{\pi} \sum_{n=0}^{\infty} \frac{(-1)^n}{(2n+1)} \frac{\sin \omega_n t}{\omega_n} \cos (2n+1)\frac{\pi x}{2L} , \tag{14}$$

and for $t > t_0$:

$$\sigma_f(x,t) = \frac{E\alpha T_0}{t_0} \frac{4}{\pi} \sum_{n=0}^{\infty} \frac{(-1)^n}{(2n+1)} \frac{\sin \omega_n t - \sin \omega_n (t - t_0)}{\omega_n} \cos (2n+1) \frac{\pi x}{2L} . \tag{15}$$

After a rearrangement of the trigonometric functions the stresses (σ_i) and (σ_f) can also be represented in terms of a fundamental wave G(x), where G(x) is now given by

$$G(x) = \frac{1}{t_0} \frac{4L}{\pi^2 c} \sum_{n=0}^{\infty} \frac{(-1)^n}{(2n+1)^2} \sin (2n+1) \frac{\pi x}{2L} . \tag{16}$$

It represents a saw-tooth function periodic in L with the amplitude (see Fig. 5):

$$G(L) = \frac{L}{2ct_0} .$$

In terms of the function G(x,t) the stresses are then described by

$$\sigma_i(x,t) = E\alpha T_0 \left[G(x + ct) - G(x - ct)\right] \qquad \text{for } 0 \le t \le t_0 , \tag{17}$$

and

$$\sigma_f(x,t) = E\alpha T_0 \left\{\left[G(x + ct) - G(x - ct)\right] - \left[G\left[x + c(t - t_0)\right] - G\left[x - c(t - t_0)\right]\right]\right\} \qquad \text{for } t > t_0 , \tag{18}$$

or

$$\sigma_f(x,t) = \sigma_i(x,t) - \sigma_i(x,t - t_0) . \tag{19}$$

The stresses $\sigma_i(x,t)$ occurring during the pulse at $0 \le t \le t_0$ [Eq. (17)] are again given by a set of two waves travelling in opposite directions. In Eq. (18) resp. Eq. (19) an additional set of waves delayed in time by t_0 is created at the end of the heat pulse with negative sign which is superimposed on the one created at the beginning of the heating at t = 0. Again, a graphical evaluation of the stresses by the superposition of the appropriate saw-tooth functions is easily possible.

As an example, the development of the stresses in time is illustrated for rapid heating ($t_0 = L/4c$) in Fig. 6, where the time is given in units of L/c.

The stresses in the centre of the rod at x = 0 are of particular interest since the largest stresses are reached there. As shown in Appendix I, they depend on the heating period t_0 in the following way: If the duration of the heat pulse t_0 is shorter than the propagation time of sound over the total target length, i.e.

$$ct_0 \leq 2L \ , \tag{20}$$

the maximal possible stress has the value

$$\sigma_{max}(0,t) = \pm E\alpha T_0 \ . \tag{21}$$

For slow heating, i.e.

$$ct_0 > 2L \ , \tag{22}$$

the maximal stress is

$$\sigma_{max}(0,t) \leq E\alpha T_0 \ 2L/ct_0 \ . \tag{23}$$

The detailed dependence of the maximum stresses on the pulse length is shown in Fig. 7. Curve (a) gives the maximal absolute central stress, which can occur during the heating-up period ($0 \leq t \leq t_0$). Curve (b) shows the stresses which are adopted after the heating ($t > t_0$). Curve (c) shows the maximum values which can occur at any time during or after the heating. Curve (d) represents the upper limits of the central stresses as given by Eqs. (21) and (23).

2.3 The partly heated rod

In this section we want to discuss briefly the case when a particle beam hits a freely suspended thin rod perpendicular to its axis so that only a part of the length $2(L - \Delta)$ symmetrical around its centre is heated (see Fig. 8). As before, we assume that the temperature distribution along the rod remains about constant during the oscillation of the stress waves and only axial stresses are considered, disregarding the radial and tangential stresses which occur at the ends of the heated part of the rod. First an instantaneous temperature rise is considered. The calculations are in principle the same as for the totally heated rod. Only the initial conditions, shown in Fig. 8, are different from the previous case, which can again be expanded in a Fourier series. Without going into detail, we quote here only the final result:

$$\begin{aligned}\sigma_0(x,t) = \frac{1}{2} \{&F(x - \Delta + ct) + F(x - \Delta - ct) \\ &+ F(x + \Delta + ct) + F(x + \Delta - ct)\} E\alpha T_0\end{aligned} \tag{24}$$

where $F(\xi)$ is again the fundamental wave (10) for an instantaneous heat pulse. The development of the stress waves in time is shown in Fig. 9.

The stress in the centre of the rod at x = 0 is

$$\sigma_0(0,t) = F(\Delta - ct) + F(\Delta + ct)E\alpha T_0 \tag{25}$$

remembering that

$$F(\xi) = -F(-\xi) \ .$$

Equation (25) yields that the central stress at x = 0 of a partly heated rod is the same as the stress in a totally heated rod at x = Δ, so that the central stresses of the case discussed here can always be obtained from the stresses derived in Section 1.1. This statement is also valid for a heat pulse of finite length, and therefore the results obtained in Section 1.2 may be used for the evaluation of the stresses considered here:

$$\sigma_i(x,t) = \frac{1}{2}\{G(x - \Delta + ct) - G(x - \Delta - ct) + G(x + \Delta + ct) - G(x - \Delta - ct)\}E\alpha T_0 \quad \text{for } 0 \leq t \leq t_0 \tag{26}$$

and

$$\sigma_f(x,t) = \sigma_i(x,t) - \sigma_i(x,t - t_0) \qquad \text{for } t_0 < t \ . \tag{27}$$

The estimate of the maximum stresses in the centre of the partly heated rod is given in Appendix I.2. Results similar to those of the totally heated rod are obtained; however, the characteristic length is now given by the length 2(L - Δ) of the heated part and no longer by the total length L of the rod. When the duration of the heat pulse is shorter than the propagation time of sound over the length of the heated part, i.e.

$$ct_0 \leq 2(L - \Delta) \ , \tag{28}$$

it is

$$\sigma_{max}(0,t) = \pm E\alpha T_0 \ , \tag{29}$$

and for long pulses with

$$ct_0 > 2(L - \Delta) \tag{30}$$

it is

$$\sigma_{max}(0,t) \leq E\alpha T_0 \ 2(L - \Delta)/ct_0 \ . \tag{31}$$

2.4 General criterion for longitudinal stress waves

If one compares the results obtained for the totally and partly heated rod, one can establish the following general rule: a characteristic criterion is the time in which the sound can traverse the region, heated by the beam. If this time is longer than the heat pulse, maximum stresses of $\pm E\alpha T_0$ occur. If the characteristic time is shorter than the heat pulse, the maximum stresses are reduced by a factor given by the ratio of the characteristic traversal time over the pulse duration.

3. STRESS WAVES IN DISKS AND CYLINDERS

3.1 Stress waves in a disk

In this section we consider stress waves, created in a thin disk of radius R, which is heated uniformly to a temperature T_0 within a central area of radius r_0, as shown in Fig. 10. Such a situation may occur when a high-energy particle beam traverses a disk at its centre.

For the calculation of stress waves in disks and cylinders (see Section 3.3) the boundary conditions at the rim have to be defined. For most applications the outer surface of the body can be considered as radially free, i.e. the radial expansion at the rim is not prevented so that the radial stress σ_r vanishes there. This boundary condition leads, however, to major mathematical complications. Therefore only the simpler case of a radially constrained body is considered, i.e. any radial displacement at the rim is prevented.

However, it can be shown that in cases where the radius of the heated zone is small compared to that of the disk ($r_0 \ll R$), as is the case for irradiated disks and cylinders, the influence of the boundary conditions given at the rim of the disk can be neglected. This is also valid for stress waves at least in the first instant before they have reached the rim of the disk. Since during further reflections the stress waves will be damped, the highest stresses will be reached during the initial period. Therefore the following estimates should give realistic upper limits for the radial and tangential stress values which occur in radially constrained as well as radially free disks. The small axial stresses may be neglected for thin disks.

Besides the stress waves due to the rapid heating, also the quasi-static thermal stresses must be taken into account which occur as long as the quasi-static non-uniform temperature field is maintained in the disk.

The quasi-static radial and tangential stresses $\bar{\sigma}_r$ resp. $\bar{\sigma}_\phi$ developed by the quasi-static temperature field, are evaluated in Appendix II. The results are shown in Fig. 11.

To facilitate the evaluation of the dynamic stresses, we consider first the quasi-static radial displacement $\bar{U}(r)$ of the disk material, created by the quasi-static temperature field (see Appendix II and Fig. 12). This quasi-static displacement $\bar{U}(r)$ is given by

$$\bar{U}(r) = \begin{cases} \frac{1+\nu}{2}\,\alpha T_0 \left[r - \frac{r_0^2}{R^2}\, r \right] & 0 \le r \le r_0 \,, \\ \frac{1+\nu}{2}\,\alpha T_0 \left[\frac{r_0^2}{r} - \frac{r_0^2}{R^2}\, r \right] & r_0 \le r \le R \,, \end{cases} \tag{32}$$

where ν is the Poisson ratio ($\nu \approx 1/3$).

This equation satisfies the obvious condition

$$\bar{U}(0) = 0 \ , \tag{33}$$

and the assumed boundary condition that any radial expansion at r = R is prevented:

$$\bar{U}(R) = 0 \ . \tag{34}$$

To study the purely dynamic effects, the displacements U(r,t) from the equilibrium quasi-static displacement $\bar{U}(r)$ have to be calculated.

The equation of motion in terms of displacements U(r,t) has the following form for a disk (see Appendix II):

$$\frac{\partial^2 U}{\partial r^2} + \frac{1}{r}\frac{\partial U}{\partial r} - \frac{U}{r^2} = \frac{1}{c_D^2}\frac{\partial^2 U}{\partial t^2} \tag{35}$$

with

$$c_D = \sqrt{\frac{E}{\rho(1-\nu^2)}} \approx \sqrt{\frac{E}{\rho}} \ . \tag{36}$$

We proceed in a similar way to that used in the discussion of the thin rod with the ansatz:

$$U(r,t) = \alpha T_0 \sum_{n=0}^{\infty} b_n(r) \cos \omega_n t \ , \tag{37}$$

which satisifies again

$$\left.\frac{\partial U}{\partial t}\right|_{t=0} = 0 \ . \tag{38}$$

Introducing Eq. (37) into Eq. (35) yields

$$\frac{\partial^2 b_n}{\partial z_n^2} + \frac{1}{z_n}\frac{\partial b_n}{\partial z_n} + b_n\left(1 - \frac{1}{z_n^2}\right) = 0 \tag{39}$$

with

$$z_n = \frac{\omega_n}{c} r \ . \tag{40}$$

The general solution of Eq. (39) is given by a Bessel-function of the first order J_1 as is expected from the cylindrical symmetry of the problem, and therefore $b_n(r)$ has the following form:

$$b_n(r) = c_n J_1(z_n) \ , \tag{41}$$

and thus

$$U(r,t) = \alpha T_0 \sum c_n J_1(z_n) \cos \omega_n t \ . \tag{42}$$

The initial and boundary conditions have again to be satisfied by the proper choice of the coefficients c_n and the frequencies ω_n. Since

$$J_1(0) = 0 \ , \tag{43}$$

the condition

$$U(0,t) \equiv 0 \tag{44}$$

is fulfilled. Since a radially constrained disk was assumed, it must be

$$U(R,t) \equiv 0 \tag{45}$$

which implies

$$J\left(\frac{\omega_n}{c} R\right) \equiv 0 \ . \tag{46}$$

The roots of the first-order Bessel functions are in good approximation given by

$$z_{0,n} \approx \pi(n + 1/4) \ , \tag{47}$$

so that the permitted frequencies are approximately

$$\omega_n \approx \frac{\pi c}{R} (n + 1/4) \ . \tag{48}$$

To find the coefficients c_n of the Fourier-Bessel expansion (42) we have to know the initial displacement $U(r,0)$ from the equilibrium quasi-static displacement $\bar{U}(r)$ [Eq. (32)]. In case of an instantaneous temperature rise we assume again that initially any radial displacement is prevented owing to the mass inertia of the disk material, i.e. the total resulting displacement U_T must vanish at $t = 0$:

$$U_T = U(r,0) + \bar{U}(r) = 0$$

or

$$U(r,0) = -\bar{U}(r) \ , \tag{49}$$

where $\bar{U}(r)$ is given by Eq. (32). The coefficients are then obtained with the help of the formula

$$c_n = \frac{2}{R^2} \frac{\int_0^R r \, J_1(z_n) U(r,0) \, dr}{J_0^2\left(\frac{\omega_n}{c} R\right)} \ . \tag{50}$$

Introducing Eq. (49) into Eq. (50) and solving the integral, which is a rather lengthy procedure and is therefore omitted here, gives finally

$$c_n = \frac{2}{\left(\frac{\omega_n}{c} R\right)^2} \frac{r_0 J_1\left(\frac{\omega_n}{c} r_0\right)}{J_0^2\left(\frac{\omega_n}{c} R\right)} \ . \tag{51}$$

We have hereby obtained the complete expression for the dynamic part of the radial displacement.

From this we can evaluate the radial and tangential stresses σ_r and σ_ϕ with the formulae [(AII.13) and (AII.14)] given in Appendix II*).

Introducing Eq. (42) into Eqs. (AII.13) and (AII.14) gives finally the dynamic stresses for an instantaneous temperature rise:

$$\sigma_{0r}(r,t) = \frac{2E\alpha T_0}{1-\nu} \sum_{n=0}^{\infty} \xi_0 \frac{J_1(\varepsilon_n \xi_0)}{J_0^2(\varepsilon_n)\varepsilon_n} \left[J_0(\varepsilon_n \xi) - (1-\nu) \frac{J_1(\varepsilon_n \xi)}{\varepsilon_n \xi} \right] \cos \varepsilon_n \theta \ , \qquad (52)$$

and

$$\sigma_{0\phi}(r,t) = \frac{2E\alpha T_0}{1-\nu} \sum_{n=0}^{\infty} \xi_0 \frac{J_1(\varepsilon_n \xi_0)}{J_0^2(\varepsilon_n)\varepsilon_n} \left[\nu J_0(\varepsilon_n \xi) + (1-\nu) \frac{J_1(\varepsilon_n \xi)}{\varepsilon_n \xi} \right] \cos \varepsilon_n \theta \ , \qquad (53)$$

with the abbreviations

$$\xi_0 = \frac{r_0}{R} \ , \quad \xi = \frac{r}{R} \ , \quad \theta = \frac{ct}{R} \ , \quad \varepsilon_n = \pi(n + 1/4) \ .$$

These formulae can again be used to evaluate the dynamic stresses when the disk is heated up by a pulse of finite length $\Theta_0 = ct_0/R$.

Applying again formula (12) one obtains for $0 \leq t \leq t_0$

$$\sigma_r(r,t) = \frac{1}{\Theta_0} \div \sum \div \left[\ldots \right] \frac{\sin \varepsilon_n \theta}{\varepsilon_n} \qquad (54)$$

$$\sigma_\phi(r,t) = \frac{1}{\Theta_0} \div \sum \div \left[\ldots \right] \frac{\sin \varepsilon_n \theta}{\varepsilon_n} \qquad (55)$$

and for $t > t_0$

$$\sigma_r(r,t) = \frac{1}{\Theta_0} \div \sum \div \left[\ldots \right] \left[\frac{\sin \varepsilon_n \theta}{\varepsilon_n} - \frac{\sin \left[\varepsilon_n (\Theta - \Theta_0) \right]}{\varepsilon_n} \right] , \qquad (56)$$

$$\sigma_\phi(r,t) = \frac{1}{\Theta_0} \div \sum \div \left[\ldots \right] \left[\frac{\sin \varepsilon_n \theta}{\varepsilon_n} - \frac{\sin \left[\varepsilon_n (\Theta - \Theta_0) \right]}{\varepsilon_n} \right] . \qquad (57)$$

The symbols used in Eqs. (54) to (57) represent the corresponding expressions in Eq. (52) and (53), respectively.

Again we find the result, already obtained for the one-dimensional case, that at the end of the pulse at $t = t_0$ a second stress wave is created with the inverse amplitude of the one from the beginning of the pulse.

3.2 Results

The numerical evaluation of the formulae (56) and (57) has been performed with a computer. To obtain the total stresses $\sigma_{T,r}(r,t)$ and $\sigma_{T,\phi}(r,t)$ one has still to add the quasi-static stresses:

---

*) For the case of a radially free disk, the dynamic stresses may be developed in a Dini series. The evaluation of the permitted ω_n satisfying $\sigma_r(R,t) \equiv 0$ is, however, more complicated.

$$\sigma_{T,r}(r,t) = \sigma_r(r,t) + \bar{\sigma}_r(r) \ ,$$

$$\sigma_{T,\phi}(r,t) = \sigma_\phi(r,t) + \bar{\sigma}_\phi(r) \ .$$

The behaviour of the total radial stress as a function of time for an instantaneous temperature rise is shown in Fig. 13 for an aluminium disk of 10 cm radius and a heated centre of 2 cm radius. It is interesting to note the large negative stresses at r = 0 obtained after a delay, which corresponds to the time during which sound propagates from the boundary of the heated region at $r = r_0$ to the centre of the disk. These central stresses are much higher than the initial stress, created at time t = 0, which represents a characteristic difference from the one-dimensional case. Precise values of these stress spikes are, however, difficult to estimate since they depend strongly on the order up to which the Fourier-Bessel series are computed. After the reflection at the centre, this stress spike travels with the velocity of sound towards the outside rim at r = R changing its amplitude and shape during its traversal. This is another principal difference to the one-dimensional case, where the shape of the stress wave remains unchanged (see Fig. 9) during its propagation.

A third difference is given by the fact that two-dimensional waves leave a wake behind them, e.g. the central stress remains never constant in time after the wave peak has been reflected from the centre, whereas in the one-dimensional case the stresses remain zero, after the wave has passed.

At the arrival of the stress spike at the rim of the disk it is reflected without changing its sign, since a radially constrained disk was assumed.

The radial and tangential stresses behave principally in the same manner.

In further calculations the maximum total stresses occurring in the centre of the disk were studied as a function of the heating period t_0. In Fig. 14 the development of the central stresses in time is shown for an instantaneous temperature rise and for a finite rise-time of 20 µsec in an aluminium disk of an outer radius R = 10 cm and a heated spot with $r_0 = 2.0$ cm.

The reduction of the central stress due to the finite length of the heat pulse is remarkable. Also the negative stress wave created at the end of the heat pulse 20 µsec later can be seen. In Fig. 15 the maximum central dynamic stresses relative to the quasi-static stresses are plotted as a function of the pulse length. It can be seen that the maximum central stresses are in very good approximation inversely proportional to the pulse length for the case when

$$t_0 > r_0/c \ .$$

In Fig. 16 the maximum central dynamic stresses relative to the quasi-static stresses are plotted as a function of the size of the heated region. They show an approximately linear dependence on the radius of the heated area.

From the correlation of the stresses to the pulse length and spot size of the heated area we may draw the following conclusion: for small heated areas, similar to the one-dimensional case, the ratio of the pulse duration and the dimension of the heated area, i.e. the propagation time of sound through this area, characterizes the contribution of dynamic effects in rapidly heated disks. This may be shown by the evaluation of Eq. (54) at $r = 0$ and $t = r_0/c$ and approximating the time dependence $1/\Theta \sin \varepsilon_n \Theta \approx \varepsilon_n$ for the case $r_0 \ll R$.

From the computer calculations, the following upper limits of the maximum central dynamic stresses were derived:

$$\sigma_{r\ max} = \sigma_{\phi\ max} \leq \frac{2r_0}{ct_0} E\alpha T_0 \quad \text{for } ct_0 > r_0 \quad \text{and} \quad r_0 \ll R \ . \tag{58}$$

The factor of 2 in relation (58) takes into account the possible additive superposition of the stress wave created at the end of the pulse. These stresses relative to the quasi-static stress given in the appendix are

$$\frac{\sigma_{r\ max}}{\bar{\sigma}_r} = \frac{\sigma_{\phi\ max}}{\bar{\sigma}_\phi} \leq \frac{4r_0}{ct_0} \ . \tag{59}$$

For short pulses with

$$ct_0 \ll r_0 \tag{60}$$

values several times higher than those of the static stresses are possible.

3.3 Stress waves in a cylinder

We assume that the central region of a radially and longitudinally constrained long cylinder is heated rapidly along its axis with a temperature constant in axial direction and with a radial distribution identical to that assumed for the previously discussed disk (see Fig. 9). A similar situation occurs when a high-energy proton beam is absorbed in a long cylindrical absorber block. The problem of a cylinder can be treated in exactly the same way as that of the disk, and we therefore omit the detailed calculations and quote only the final results. The axial stresses σ_z must, of course, now be taken into account.

The static stresses and the radial displacement in a cylinder are given in Appendix III.

The radial displacement [Eq. (AIII.8)] differs from the corresponding equation for the disk (AII.7) only by the factor $1/(1 - \nu)$. The equation of motion is similar to the one for the disk [see Eq. (AIII.12)], since no waves in axial

direction are created. The solution of the differential equation with the boundary condition

$$U(0,t) = U(R,t) = 0$$

and the initial condition

$$U(r,0) = -\bar{U}(r)$$

[see Appendix, Eq. (AIII.8)] leads finally to the dynamic stresses when the relations between the stresses and the displacement for a cylinder [Appendix, Eqs. (AIII.9) - (AIII.11)] are used.

For an instantaneous temperature rise we obtain

$$\sigma_{0r}(r,t) = \frac{2E\alpha T_0}{(1+\nu)(1-2\nu)} \sum_{n=0}^{\infty} \xi_0 \frac{J_1(\varepsilon_n\xi_0)}{J_0^2(\varepsilon_n)\varepsilon_n} \left\{ J_0(\varepsilon_n\xi) - \frac{(1-2\nu)}{(1-\nu)} \frac{J_1(\varepsilon_n\xi)}{\varepsilon_n\xi} \right\} \cos \varepsilon_n\theta \tag{61}$$

$$\sigma_{0\phi}(r,t) = \frac{2E\alpha T_0}{(1+\nu)(1-2\nu)} \sum_{n=0}^{\infty} \xi_0 \frac{J_1(\varepsilon_n\xi_0)}{J_0^2(\varepsilon_n)\varepsilon_n} \left\{ \frac{\nu}{1-\nu} J_0(\varepsilon_n\xi) + \frac{(1-2\nu)}{(1-\nu)} \frac{J_1(\varepsilon_n\xi)}{\varepsilon_n\xi} \right\} \cos \varepsilon_n\theta \tag{62}$$

$$\sigma_{0z}(r,t) = \frac{2E\alpha T_0}{(1+\nu)(1-2\nu)} \sum_{n=0}^{\infty} \xi_0 \frac{J_1(\varepsilon_n\xi_0)}{J_1^2(\varepsilon_n)\varepsilon_n} \left\{ \frac{\nu}{1-\nu} J_0(\varepsilon_n\xi) \right\} \cos \varepsilon_n\theta \,. \tag{63}$$

To obtain the equations for the dynamic stresses, created by a heat pulse of finite length, Eqs. (61) to (63) have each to be multiplied by the factor $1/\Theta_0$ and the last cos-term must be replaced by

$$\frac{\sin(\varepsilon_n\theta)}{\theta} \quad \text{for } 0 \le t \le t_0$$

and by

$$\frac{\sin \varepsilon_n\theta - \sin\left[\varepsilon_n(\Theta - \Theta_0)\right]}{\theta} \quad \text{for } t_0 < t \,.$$

Since the formulae obtained for stresses in a cylinder, have the same structure as Eqs. (54) to (57) for a disk, the behaviour of waves in a cylinder and in a disk are rather similar. The absolute stress values are, however, larger since axial expansion is prevented, whereas the axial stress in a disk can be neglected. The maximum central dynamic stresses have again been evaluated numerically with a computer program. For $ct_0 > r_0$ and $r_0 \ll R$,

$$\sigma_{r\ max} = \sigma_{\phi\ max} \leq \frac{9}{2} \frac{r_0}{ct_0} E\alpha T_0 \ , \tag{64}$$

$$\sigma_{z\ max} \leq 3 \frac{r_0}{ct_0} E\alpha T_0 \ , \tag{65}$$

or relative to the corresponding static stresses,

$$\frac{\sigma_{r\ max}}{\bar{\sigma}_r} = \frac{\sigma_{\phi\ max}}{\bar{\sigma}_\phi} \leq 6 \frac{r_0}{ct_0} \ , \tag{66}$$

$$\frac{\sigma_{z\ max}}{\bar{\sigma}_z} \leq 4 \frac{r_0}{ct_0} \ . \tag{67}$$

For rapid heating with

$$ct_0 << r_0 \ ,$$

again extremely high stresses may occur. It is no longer possible to establish an easy relation for quick estimates since the maximum stresses depend strongly on the surface size of the heated area and the length of the heat pulse, so that for detailed studies a numerical evaluation of the formulae (61) to (63) is necessary.

3.4 Example

Applying the results, obtained above for the evaluation of the dynamic stresses which can be produced by a proton pulse extracted from the SPS, we assume a pulse length t_0 = 23 μsec and a heated area of about 1 cm diameter[3] in the centre of a large aluminium absorber block. In this case the velocity of sound is about

$$c \simeq 5 \times 10^5 \text{ cm/sec} \ ,$$

and the condition $ct_0 > r_0$ is fulfilled since the pulse length is longer than the traversal of sound over the heated region. Therefore the maximum dynamic stress relative to the quasi-static stresses, obtained by formulae (66) and (67) are

$$\frac{\sigma_{r\ max}}{\bar{\sigma}_r} = \frac{\sigma_{\phi\ max}}{\bar{\sigma}_\phi} \leq 24\%$$

and

$$\frac{\sigma_{z\ max}}{\bar{\sigma}_z} \leq 16\% \ .$$

The values obtained by direct computer calculations for these parameters are about 20% resp. 10%. These latter values are lower, since the stress wave created at the beginning of the pulse does not interfere constructively with the one created at the end of the pulse after 23 μsec, as was assumed in the estimates given above.

Since the velocity of sound in other materials, such as Cu or Fe which might be used as absorber material as well, is similar to the velocity of sound in Al, the preceding estimate of the relative dynamic stresses applies as well for these materials.

4. CONCLUSION

The maximum stresses to be expected in the uniformly heated external targets of the SPS are given by the value $\pm E\alpha T_0$ for long targets and short burst lengths t_0, if the stress wave created at both target ends cannot traverse the total target of length 2L during the duration of the burst. For shorter targets resp. longer bursts, the maximum stresses decrease with the ratio of the traversal time of sound over the burst length:

$$\sigma_{max} = \pm E\alpha T_0 \; 2L/ct_0 \; .$$

The most straightforward method of reducing the dynamic stresses in targets is, of course, to use several rods of reduced length placed adjacent to each other. Lengths of several centimetres are largely sufficient for the external SPS targets[4].

For cases when only part of the rod is heated instantaneously, as may occur when supports of beam observation equipment are accidentally irradiated, the parameters characterizing the stress are the width of the heated region and the burst length.

The dynamic stress in an aluminium rod irradiated sideways by a beam of 2 mm diameter and 23 μsec duration is reduced to 2% of the stress produced with instantaneous heating. For an alumina-rod, commonly used in beam observation equipment for electric isolation purposes, the corresponding value is only 1%. The materials may, however, fail owing to the static stresses produced by the non-uniform temperature field or even owing to melting of the material, depending on the beam energy and intensity.

For larger beam cross-sections, even smaller dynamic stresses are expected since the maximum temperature decreases about quadratically with the width of the heated area, whereas the dynamic stresses increase only linearly with the width of the heated region.

For the partly heated rod one may therefore conclude that the dynamic stresses can be neglected as long as the traversal time of sound across the irradiated and therefore heated region is small compared with the burst length. This will in general be the case as long as the beam traverses the rod perpendicular to its axis.

Regarding the situation where a disk or a cylinder is irradiated along its axis, the temperature will only increase considerably in a region of about 1 cm diameter[3] or less. Therefore, arguments similar to the one given for the partly heated rod apply also for irradiated disks and cylinders and extreme stresses occurring with instantaneous heating do not have to be expected for bursts of 23 μsec duration. Consequently, the stresses may be estimated by relation (58) resp. (66) and (67). According to these formulae the dynamic stresses will in most cases be below 30% of the accompanying quasi-static stress, produced by the considered quasi-static temperature field in disks and cylinders.

Therefore, regarding stresses produced by the SPS beam, the first approach should always be the evaluation of the static stresses to which thereafter the dynamic stresses may be added as a correction.

For shorter particle bursts however, the dynamic stresses may exceed by far the static ones, and the numerical evaluation of the derived formulae becomes necessary.

Acknowledgements

The author wishes to thank all colleagues who through stimulating discussions have contributed to this paper. In particular, he would like to thank H. Bargmann and W.C. Middelkoop for their constant interest and many useful remarks. The efficient handling of the manuscript by the CERN Typing Service is gratefully acknowledged.

REFERENCES

1) H. Bargmann, Dynamic response of external targets under thermal shock, CERN-Lab II/BT/Int/73-3 (1973).

2) R.T. Avery, D. Keefe, T.L. Brekke and I. Finnie, Shattering rock with intense bursts of energetic electrons, IEEE Trans. Nuclear Sci. NS-20, No. 3, 1010-1014 (1973).

3) K. Teutenberg, P. Sievers and W.C. Middelkoop, Beam dump absorber blocks for the internal and external beam lines of the SPS, CERN-Lab II/BT/74-4 (1974).

4) W. Kalbreier, W.C. Middelkoop and P. Sievers, External targets at the SPS, CERN-Lab II/BT/74-1 (1974).

5) S.P. Timoshenko and J.N. Goodier, Theory of elasticity (3rd edition) (McGraw-Hill, Inc., New York, 1970).

APPENDIX I

THE MAXIMAL CENTRAL STRESSES

I.1 The maximal central stresses in the totally heated rod

The central stresses at x = 0 during the heat pulse, i.e.

$$0 \leq t \leq t_0 \ .$$

are obtained from Eq. (17) in Section 2.2:

$$\sigma_i(0,t) = E\alpha T_0\{G(ct) - G(-ct)\} \ . \tag{AI.1}$$

Since

$$G(\xi) = -G(-\xi) \tag{AI.2}$$

it follows that

$$\sigma_i(0,t) = 2G(ct)E\alpha T_0 \ . \tag{AI.3}$$

If the heating-up period is shorter than the time, the sound needs to travel from the end of the rod x = L to the centre x = 0, i.e.

$$ct_0 \leq L \ , \tag{AI.4}$$

the fundamental wave is (see Fig. 5)

$$G(\xi) = \frac{\xi}{2ct_0} \quad \text{for } 0 \leq \xi \leq L \ . \tag{AI.5}$$

It follows immediately from Eqs. (AI.3) and (AI.5)

$$\sigma_i(0,t) = \frac{t}{t_0} E\alpha T_0 \ . \tag{AI.6}$$

The central stress is growing linearly in time, until its maximum is reached at the end of the pulse at $t = t_0$, where the stress becomes

$$\sigma_i(0,t_0) = E\alpha T_0 \ . \tag{AI.7}$$

This result is in agreement with Ref. 1. For larger heating periods with

$$ct_0 > L \ , \tag{AI.8}$$

where the propagation time of sound for the length L of the rod is shorter than the heat pulse t_0, the maximum central stress during the pulse is reached (see Fig. 5) for

$$ct = L \ , \tag{AI.9}$$

where G(ct) has a maximum.

For longer heat pulses, satisfying condition (AI.8) the maximum stress is

$$\sigma_i(0,L/c) = 2G(L)E\alpha T_0 = \frac{L}{t_0 c} E\alpha T_0 \ . \qquad \text{(AI.10)}$$

The stress is proportional to the ratio of the rod length over the pulse duration.

Up to now we have only considered the stresses $\sigma_i(x,t)$ occuring during the heating. As shown by Eq. (19), an additional stress wave with negative amplitude is created at $t = t_0$ owing to the "switching off" of the heat pulse. This stress wave may interfere constructively or destructively with the initial stress wave, depending on its phase at the time, when the second one is initiated. In particular it may happen that the delayed stress wave doubles the initial stress amplitude or that it cancels it out completely. Disregarding the detailed dependence on the pulse length, the maximum possible stresses may be estimated in the following way:

For pulse lengths

$$t_0 > \frac{2L}{c} \ . \qquad \text{(AI.11)}$$

it is

$$\sigma_{max}(0,t) \leq E\alpha T_0 \ 2L/ct_0 \ , \qquad \text{(AI.12)}$$

where the factor of 2 is due to the possible constructive superposition of the stress waves from the pulse start and the pulse stop. For

$$t_0 < \frac{2L}{c} \qquad \text{(AI.13)}$$

it is

$$\sigma_{max}(0,t) = E\alpha T_0 \ . \qquad \text{(AI.14)}$$

I.2 The maximum central stresses in the partly heated rod

The central stress can be obtained from Eqs. (26) and (27):

$$\sigma_i(0,t) = E\alpha T_0\{G(\Delta + ct) - G(\Delta - ct)\} \quad \text{for } 0 \leq t \leq t_0 \qquad \text{(AI.15)}$$

$$\sigma_f(0,t) = \sigma_i(0,t) - \sigma_i(0,t - t_0) \quad \text{for } t_0 < t \ . \qquad \text{(AI.16)}$$

For pulse durations with

$$\Delta + ct_0 \leq L \text{ resp. } t_0 \leq \frac{L - \Delta}{c} \qquad \text{(AI.17)}$$

i.e. the pulse is shorter than the characteristic time for sound to propagate from the boundary of the heated part at $x = (L - \Delta)$ to the centre at $x = 0$, it is (see Fig. 5)

$$G(\xi) = \frac{\xi}{2t_0 c} \, . \tag{AI.18}$$

The stresses at x = 0 for pulse lengths satisfying (AI.17) then become

$$\sigma_i(0,t) = \frac{t}{t_0} \, E\alpha T_0 \, , \tag{AI.19}$$

and in particular the maximum value, reached at $t = t_0$, is again

$$\sigma_{max}(0,t) = E\alpha T_0 \, . \tag{AI.20}$$

Relation (AI.20) holds also for longer pulses with $t_0 \leq 2(L - \Delta)/c$, similar to the case of the totally heated rod, since the second stress wave created when the pulse is switched off can be superimposed constructively to the first wave initiated at the pulse start. For longer pulses with

$$t_0 > \frac{2(L - \Delta)}{c} \, , \tag{AI.21}$$

again a useful estimate of the maximum possible stresses is

$$\sigma_{max}(0,t) \leq \frac{2(L - \Delta)}{t_0 c} \, E\alpha T_0 \, . \tag{AI.22}$$

In this case the maximum possible stresses increase with the ratio of the length of the heated part over the pulse duration.

APPENDIX II

STRESSES IN A DISK

The static thermal stresses in a radially constrained disk of outside radius R are given by[5)]

$$\bar{\sigma}_r = E\alpha \left\{ \frac{1}{r^2} \int_0^r T\, r\, dr + \frac{(1+\nu)}{(1-\nu)} \frac{1}{R^2} \int_0^R T\, r\, dr \right\} \tag{AII.1}$$

$$\bar{\sigma}_\phi = E\alpha \left\{ -\frac{1}{r^2} \int_0^r T\, r\, dr + \frac{(1+\nu)}{(1-\nu)} \frac{1}{R^2} \int_0^R T\, r\, dr + T \right\}, \tag{AII.2}$$

where

E is the modulus of elasticity

α is the coefficient for thermal expansion

ν is the Poisson ratio.

The radial displacement is

$$\bar{U}_r = (1+\nu)\,\alpha \left\{ \frac{1}{r} \int_0^r T\, r\, dr - \frac{r}{R^2} \int_0^R T\, r\, dr \right\} . \tag{AII.3}$$

As temperature distribution it is assumed that

$$T = \begin{cases} T_0 & 0 \le r \le r_0 \\ 0 & r_0 \le r \le R \end{cases} . \tag{AII.4}$$

Introducing formulae (AII.4) into the above equations give

$$\bar{\sigma}_r = \begin{cases} \frac{E\alpha T_0}{2} \left[1 + \frac{r_0^2}{R^2} \frac{(1+\nu)}{(1-\nu)} \right] & 0 \le r \le r_0 \\ \frac{E\alpha T_0}{2} \left[\frac{r_0^2}{r^2} + \frac{r_0^2}{R^2} \frac{(1+\nu)}{(1-\nu)} \right] & r_0 \le r \le R \end{cases} \tag{AII.5}$$

$$\bar{\sigma}_\phi = \begin{cases} \frac{E\alpha T_0}{2} \left[1 + \frac{r_0^2}{R^2} \frac{(1+\nu)}{(1-\nu)} \right] & 0 \le r \le r_0 \\ \frac{E\alpha T_0}{2} \left[-\frac{r_0^2}{r^2} + \frac{r_0^2}{R^2} \frac{(1+\nu)}{(1-\nu)} \right] & r_0 \le r \le R . \end{cases} \tag{AII.6}$$

$$\bar{U} = \begin{cases} \frac{1+\nu}{2} \alpha T_0 \left[r - \frac{r_0^2}{R^2} r \right] & 0 \le r \le r_0 \\ \frac{1+\nu}{2} \alpha T_0 \left[\frac{r_0^2}{r} - \frac{r_0^2}{R^2} r \right] & r_0 \le r \le R . \end{cases} \tag{AII.7}$$

For

$$r_0 \ll R$$

the stresses are approximately given by

$$\bar{\sigma}_r = \begin{cases} \frac{E\alpha T_0}{2} & 0 \le r \le r_0 \\ \frac{E\alpha T_0}{2} \frac{r_0^2}{r^2} & r_0 \le r \le R \end{cases} \tag{AII.8}$$

$$\bar{\sigma}_\phi = \begin{cases} \frac{E\alpha T_0}{2} & 0 \le r \le r_0 \\ -\frac{E\alpha T_0}{2} \frac{r_0^2}{r^2} & r_0 \le r \le R \, . \end{cases} \tag{AII.9}$$

For

$$r_0 \ll R$$

the central stresses at r = 0 are then given by

$$\bar{\sigma}_r(0) = \frac{E\alpha T_0}{2} \tag{AII.10}$$

$$\bar{\sigma}_\phi(0) = \frac{E\alpha T_0}{2} \, . \tag{AII.11}$$

The equation of equilibrium in a disk is given by

$$\frac{\partial \sigma_r}{\partial r} + \frac{\sigma_r - \sigma_\phi}{r} = \rho \frac{\partial^2 U}{\partial t^2} \, . \tag{AII.12}$$

Since the displacements U and the stresses σ are correlated by

$$\sigma_r = \frac{E}{1 - \nu^2} \left[\frac{\partial U}{\partial r} + \nu \frac{U}{r} \right] \tag{AII.13}$$

$$\sigma_\phi = \frac{E}{1 - \nu^2} \left[\frac{U}{r} + \nu \frac{\partial U}{\partial r} \right] \tag{AII.14}$$

it follows that

$$\frac{\partial^2 U}{\partial r^2} + \frac{1}{r} \frac{\partial U}{\partial r} - \frac{U}{r^2} = \frac{1}{c_D^2} \frac{\partial^2 U}{\partial t^2} \tag{AII.15}$$

$$c_D = \sqrt{\frac{E}{\rho(1 - \nu^2)}} \approx \sqrt{\frac{E}{\rho}} \, . \tag{AII.16}$$

APPENDIX III

STRESSES IN A CYLINDER

The stresses for a longitudinally and radially constrained cylinder are

$$\bar{\sigma}_r = \frac{E\alpha}{1-\nu}\left[\frac{1}{r^2}\int_0^r T\,r\,dr + \frac{1}{1-2\nu}\frac{1}{R^2}\int_0^R T\,r\,dr\right] \tag{AIII.1}$$

$$\bar{\sigma}_\phi = \frac{E\alpha}{1-\nu}\left[-\frac{1}{r^2}\int_0^r T\,r\,dr + \frac{1}{1-2\nu}\frac{1}{R^2}\int_0^R T\,r\,dr + T\right] \tag{AIII.2}$$

$$\bar{\sigma}_z = \frac{E\alpha}{1-\nu}\left[\frac{2\nu}{1-2\nu}\frac{1}{R^2}\int_0^R T\,r\,dr + T\right]. \tag{AIII.3}$$

With the assumed temperature distribution

$$T(r) = \begin{cases} T_0 & 0 \le r \le r_0 \\ 0 & r_0 \le r \le R \end{cases} \tag{AIII.4}$$

the stresses become

$$\bar{\sigma}_r = \begin{cases} \frac{E\alpha T_0}{2(1-\nu)}\left[1 + \frac{r_0^2}{R^2}\frac{1}{1-2\nu}\right] & 0 \le r \le r_0 \\ \frac{E\alpha T_0}{2(1-\nu)}\left[\frac{r_0^2}{r^2} + \frac{r_0^2}{R^2}\frac{1}{1-2\nu}\right] & r_0 \le r \le R \end{cases} \tag{AIII.5}$$

$$\bar{\sigma}_\phi = \begin{cases} \frac{E\alpha T_0}{2(1-\nu)}\left[1 + \frac{r_0^2}{R^2}\frac{1}{1-2\nu}\right] & 0 \le r \le r_0 \\ \frac{E\alpha T_0}{2(1-\nu)}\left[-\frac{r_0^2}{r^2} + \frac{r_0^2}{R^2}\frac{1}{1-2\nu}\right] & r_0 \le r \le R \end{cases} \tag{AIII.6}$$

$$\bar{\sigma}_z = \begin{cases} \frac{E\alpha T_0}{1-\nu}\left[1 + \frac{r_0^2}{R^2}\frac{\nu}{1-2\nu}\right] & 0 \le r \le r_0 \\ \frac{E\alpha T_0}{1-\nu}\left[\frac{r_0^2}{R^2}\frac{\nu}{1-2\nu}\right] & r_0 \le r \le R\,. \end{cases} \tag{AIII.7}$$

The radial displacement is

$$\bar{U}(r) = \begin{cases} \frac{1+\nu}{2(1-\nu)}\alpha T_0\left[r - \frac{r_0^2}{R^2}r\right] & 0 \le r \le r_0 \\ \frac{1+\nu}{2(1-\nu)}\alpha T_0\left[\frac{r_0^2}{r} - \frac{r_0^2}{R^2}r\right] & r_0 \le r \le R\,. \end{cases} \tag{AIII.8}$$

The stress-strain relations for a cylinder are

$$\sigma_r = \frac{(1 - \nu)}{(1 + \nu)(1 - 2\nu)} E \left[\frac{\partial U}{\partial r} + \frac{\nu}{1 - \nu} \frac{U}{r}\right] \tag{AIII.9}$$

$$\sigma_\phi = \frac{(1 - \nu)}{(1 + \nu)(1 - 2\nu)} E \left[\frac{U}{r} + \frac{\nu}{1 + \nu} \frac{\partial U}{\partial r}\right] \tag{AIII.10}$$

$$\sigma_z = \frac{\nu}{(1 + \nu)(1 - 2\nu)} E \left[\frac{\partial U}{\partial r} + \frac{U}{r}\right] . \tag{AIII.11}$$

The equation of motion is given by

$$\frac{\partial^2 U}{\partial r^2} + \frac{1}{r} \frac{\partial U}{\partial r} - \frac{U}{r^2} = \frac{1}{c_C} \frac{\partial^2 U}{\partial t^2} \tag{AIII.12}$$

$$c_C = \sqrt{\frac{E(1 - \nu)}{\rho(1 + \nu)(1 - 2\nu)}} . \tag{AIII.13}$$

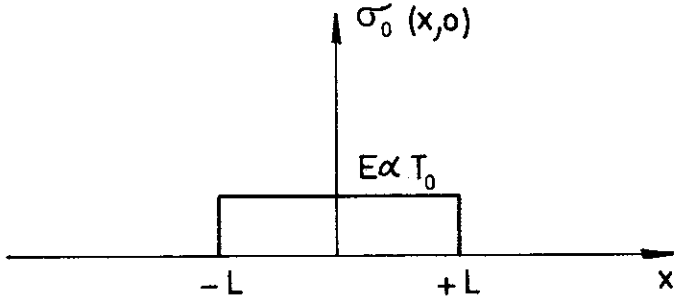

Fig. 1 Initial axial stress distribution in an instantaneously heated rod.

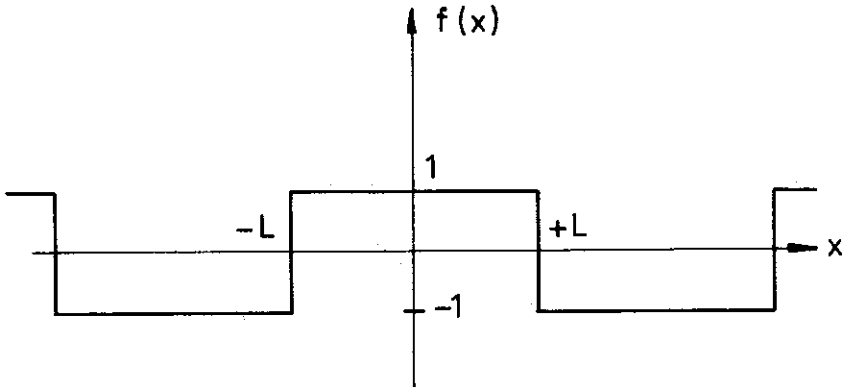

Fig. 2 The square wave describing the initial axial stress distribution in the rod $-L \leq x \leq +L$.

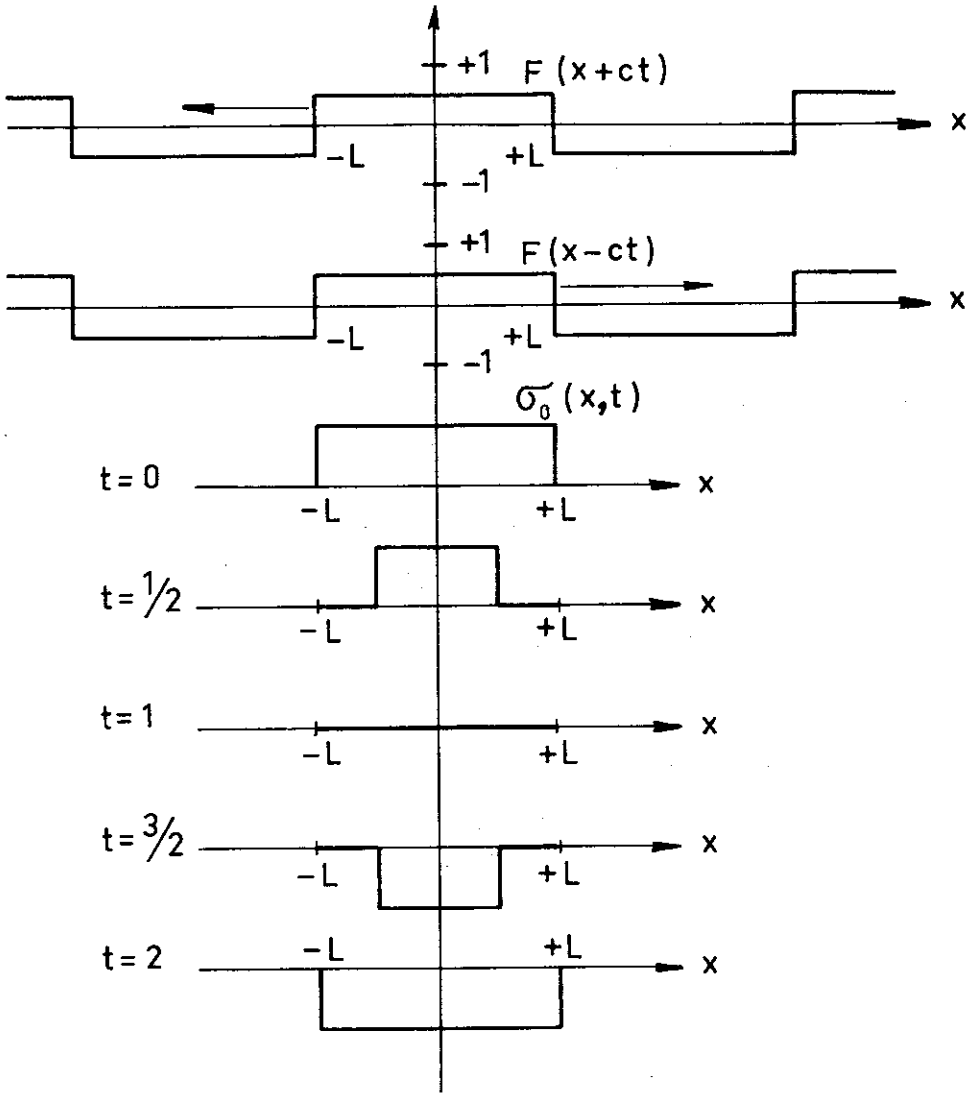

Fig. 3 The development of the axial stress in the instantaneously heated rod, obtained by the superposition of two square waves F(x,t), travelling in opposite directions. The time t is measured in units of L/c.

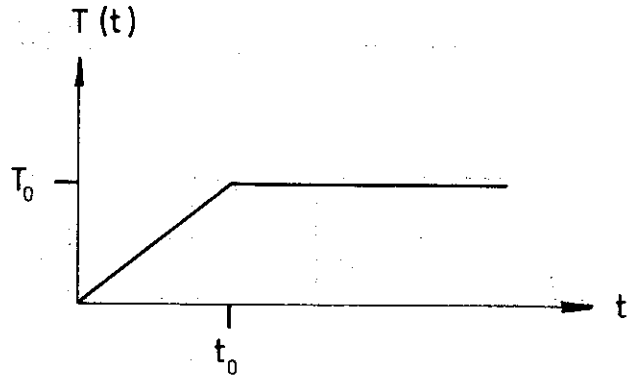

Fig. 4 The time dependence of the temperature in a rod heated by a particle burst of duration t_0.

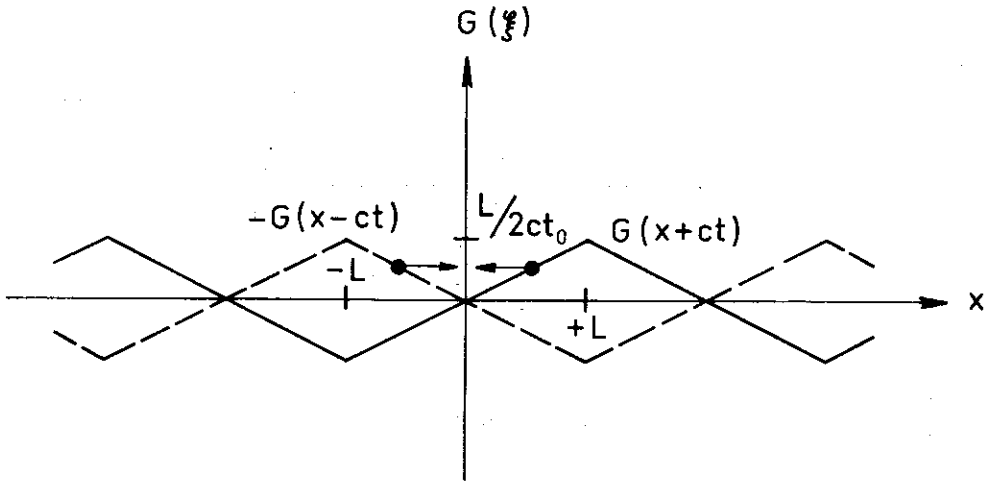

Fig. 5 The saw-tooth functions travelling in opposite directions and constituting the stresses in a rod, heated by a particle burst of duration t_0.

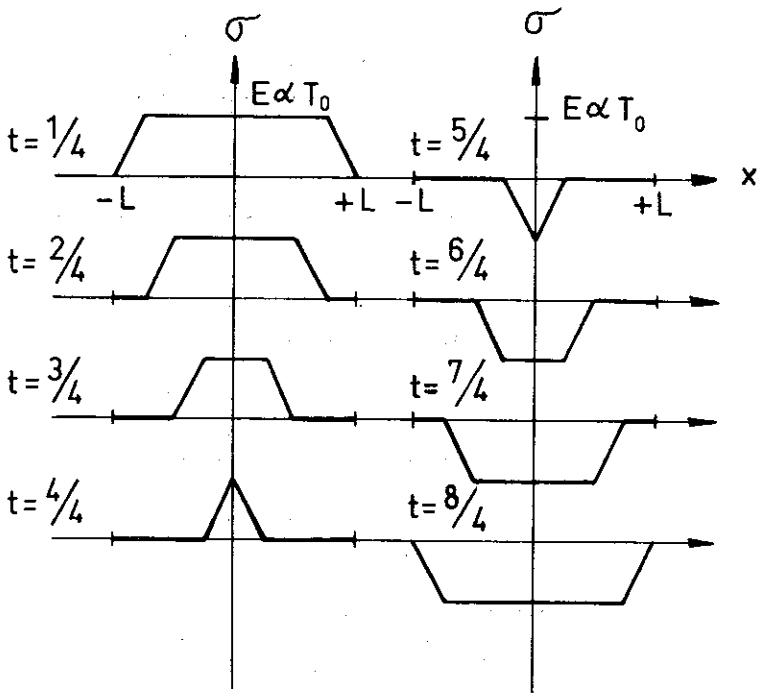

Fig. 6 The development of the axial stress in the rod, heated by a particle burst of duration $t_0 = L/4c$. The time t is measured in units of L/c.

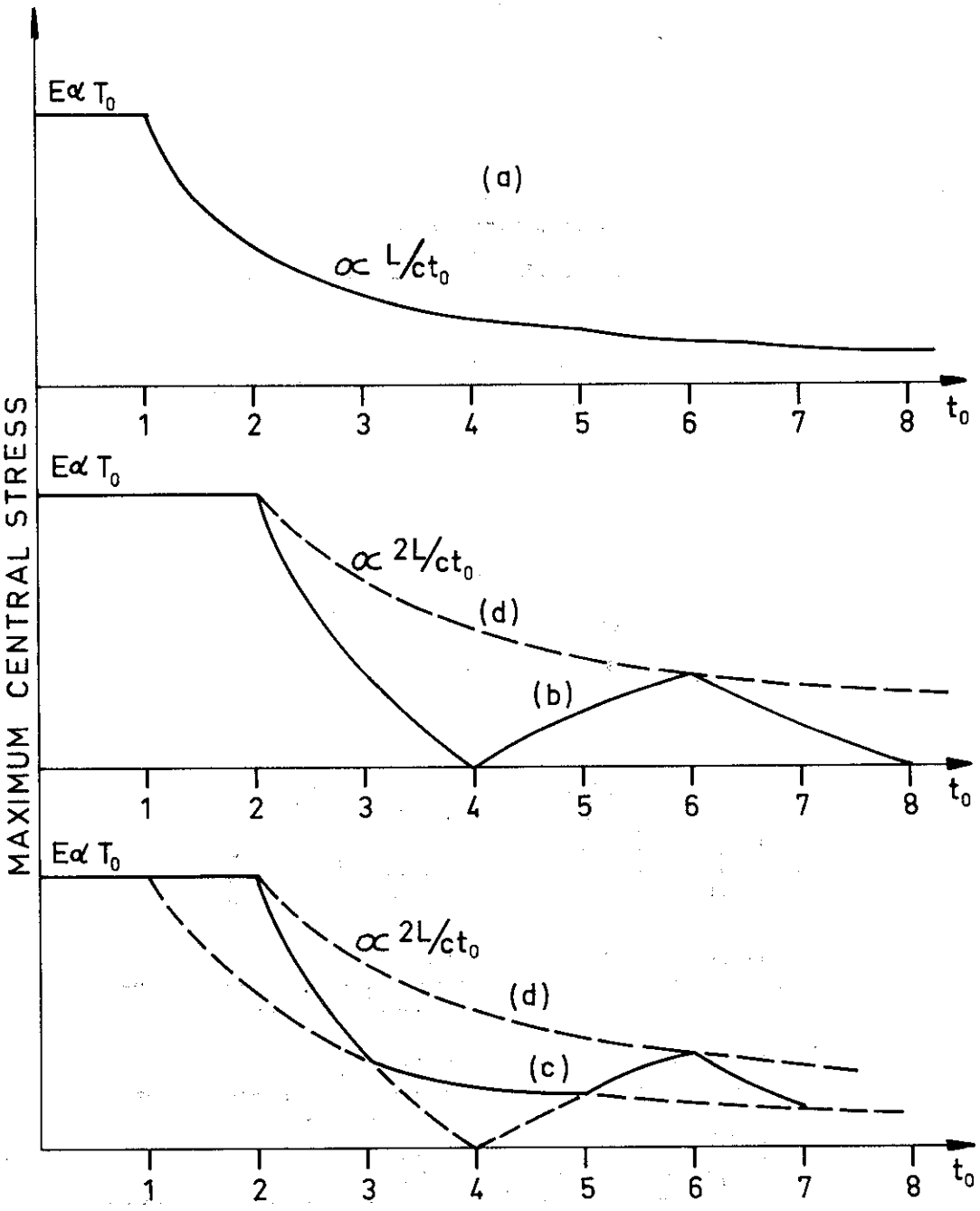

Fig. 7 The maximum absolute axial stresses in the centre of the rod as a function of the burst length obtained:

a) during the heating period t_0,

b) after the heating period t_0,

c) during or after the heating period t_0.

Curve (d) gives the upper limit of the possible stresses. The burst length t_0 is given in units of L/c.

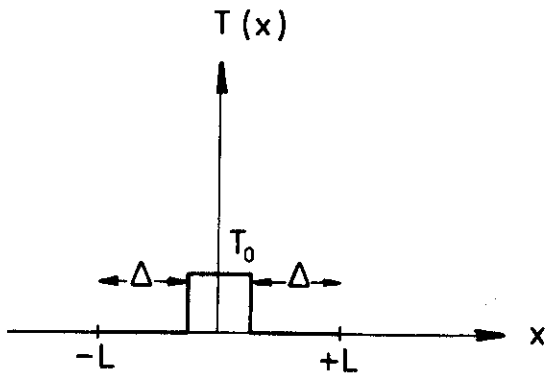

Fig. 8 Assumed temperature distribution for an instantaneously and partly heated rod.

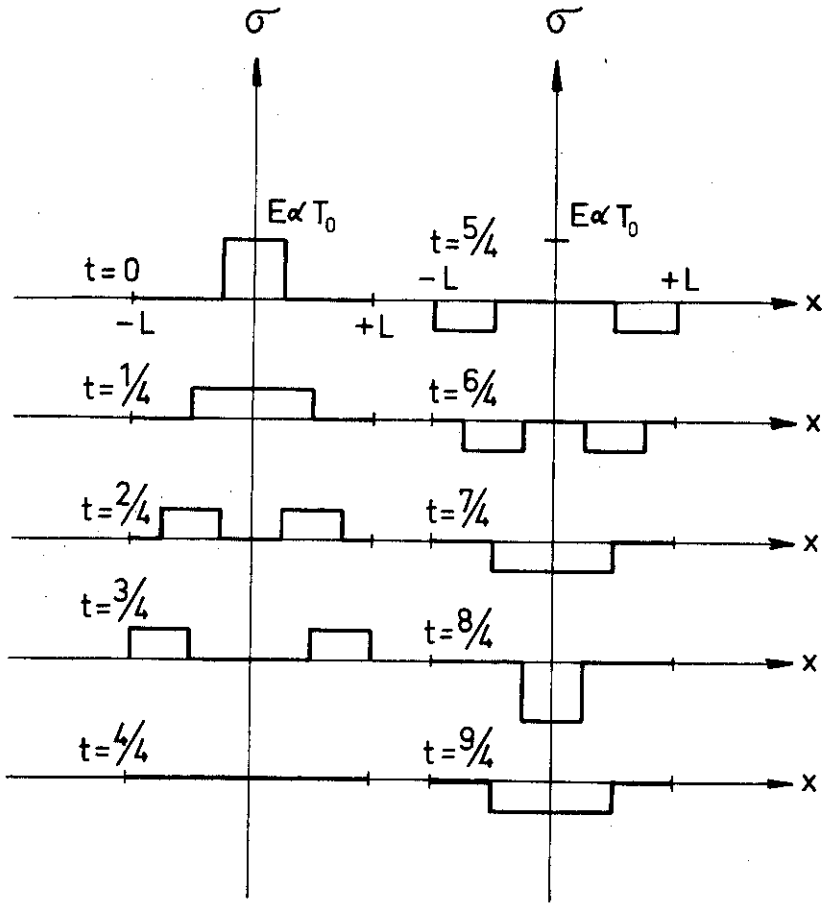

Fig 9 Development of the axial stresses in an instantaneously and partly heated rod. The time parameters are given in units of L/c.

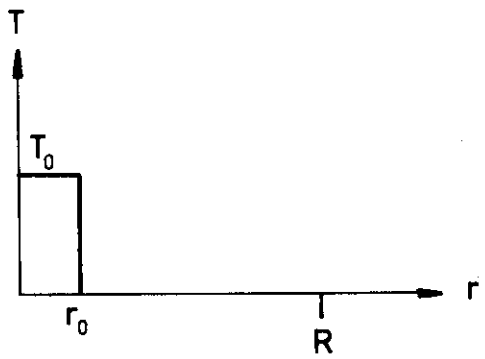

Fig. 10 Assumed radial temperature distribution for a partly heated disk.

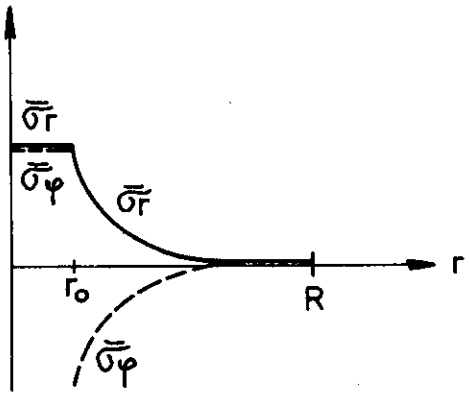

Fig. 11 The quasi-static thermal stresses in radial and tangential direction, produced by the assumed temperature field.

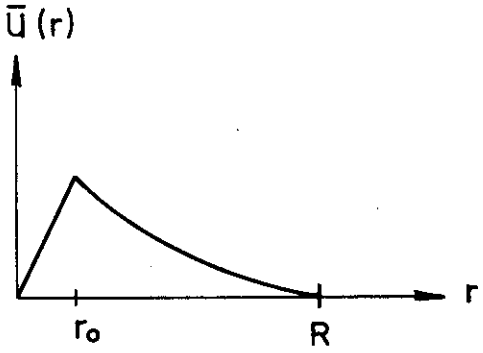

Fig. 12 The quasi-static radial displacement produced by the assumed temperature field.

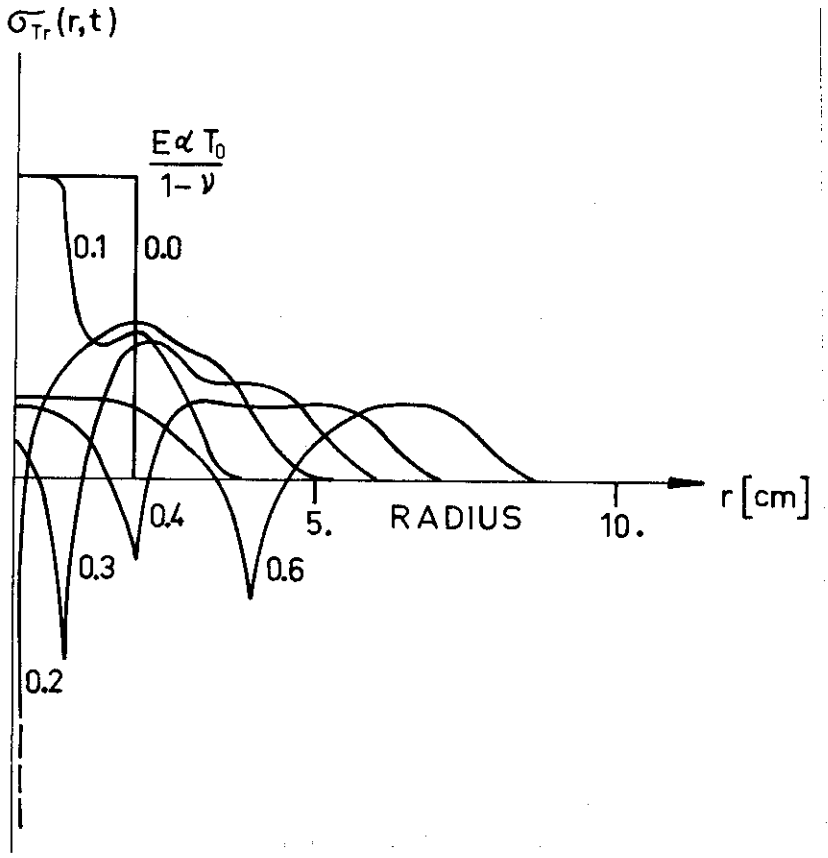

Fig. 13 The total (quasi-static plus dynamic) radial stress in an instantaneously heated Al disk of radius R at different times. The time parameters are given in units of R/c.

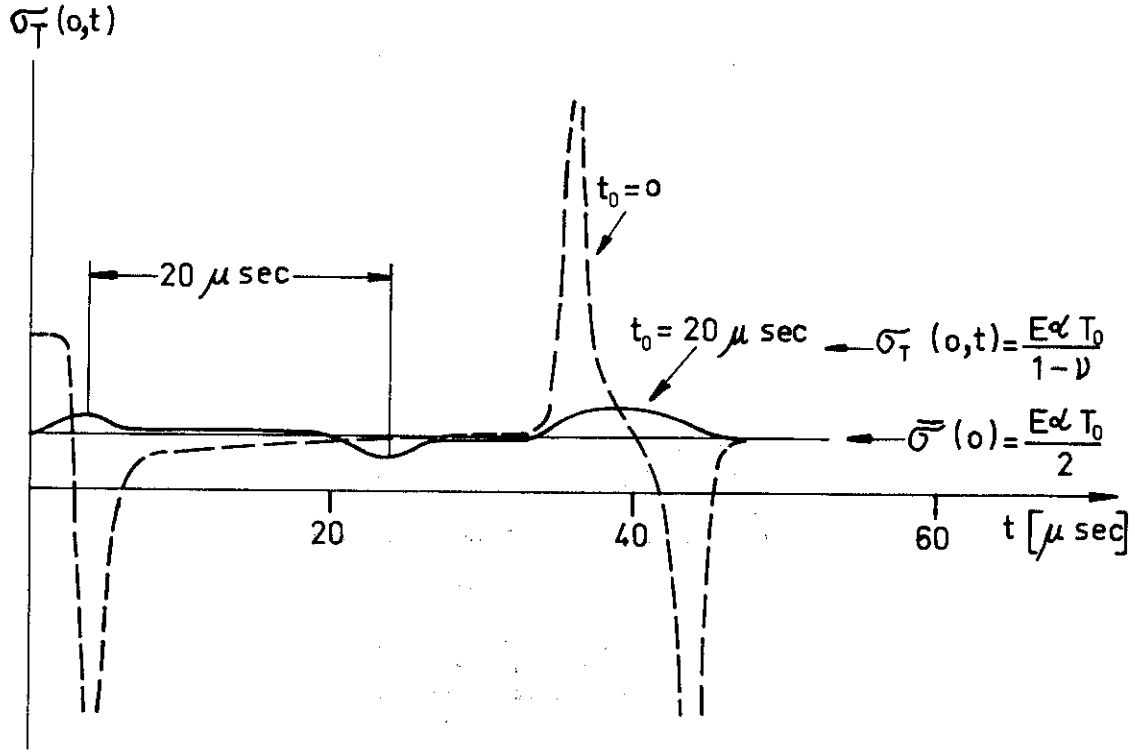

Fig. 14 The development of the total central stress in time for an infinitely rapid (t_0 = 0) and a finite (t_0 = 20 μsec) temperature increase.

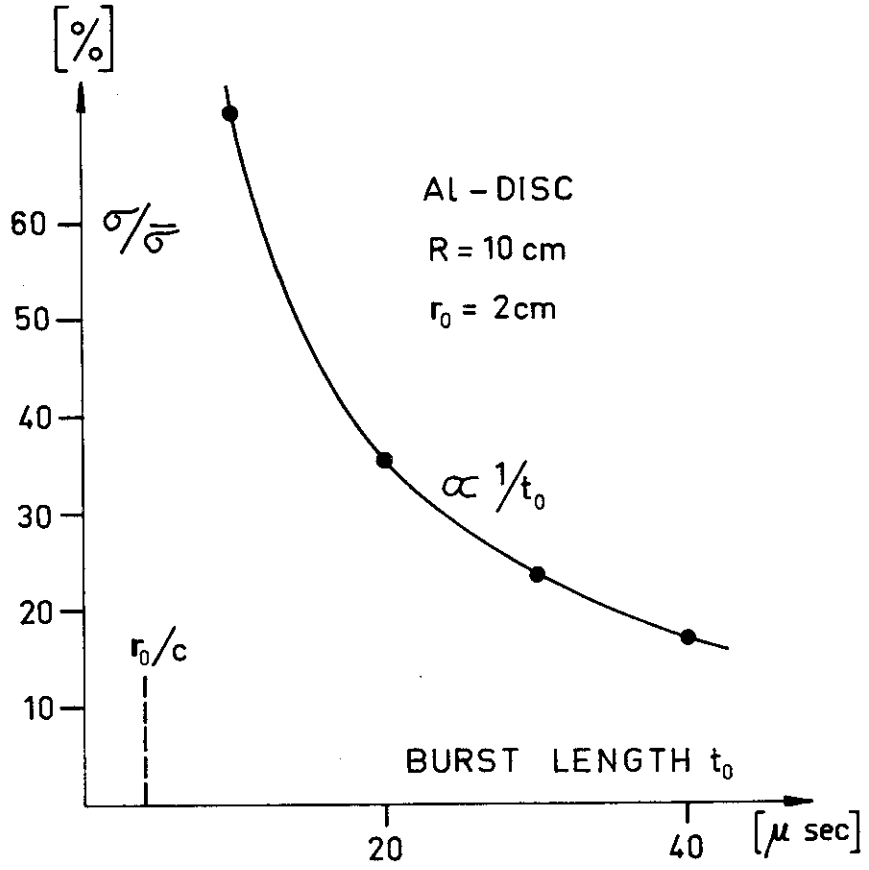

Fig. 15 The maximum central dynamic stress, normalized on the corresponding quasi-static stress, as a function of the burst length t_0.

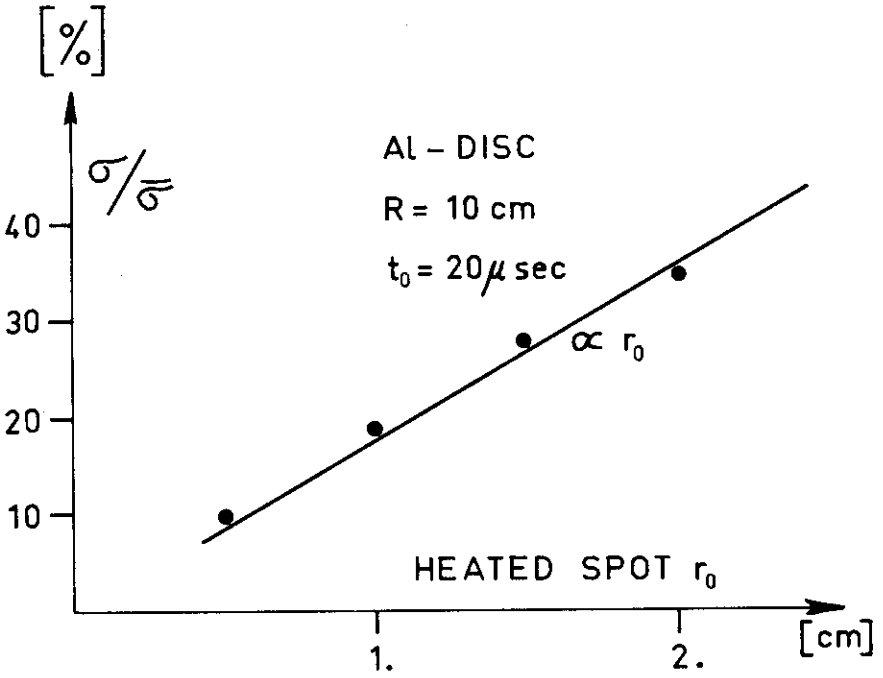

Fig. 16 The maximum central dynamic stress, normalized on the corresponding quasi-static stress, as a function of the radius of the heated area r_0.